Electronic Requirements for Oxygen Atom Transfer from Alkyl Hydroperoxides. Model Studies on Multisubstrate Flavin-Containing Monooxygenases

Robert D. Bach* and Olga Dmitrenko

Department of Chemistry and Biochemistry, University of Delaware, Newark, Delaware 19716

Received: May 10, 2003; In Final Form: August 9, 2003

Density functional calculations at the B3LYP/6-31+G(d,p) level are used to study the mechanism of 4a-hydroperoxyflavin oxidation of a series of heteroatom nucleophiles. The oxidation of xenobiotics catalyzed by flavin-containing monooxygenases (FMOs) is modeled by the oxidation of N-, S-, P-, and Se-containing nucleophiles. A mechanism for distinguishing oxygen atom versus hydroxyl transfer from RO−OH to $(CH_3)_3N$, $(CH_3)_2S$, $(CH_3)_3P$, and $(CH_3)_2Se$ is presented. The nature of these oxidative processes is related to the magnitude of the single imaginary frequency for the transition state for oxygen atom transfer. Classical activation barriers for oxygen atom transfer from a tricyclic isoalloxazine C-4a-hydroperoxide **3** (FlHOOH) to dimethyl sulfide, trimethylamine, trimethylphosphine, and dimethylselenide suggest that the reactivity of this biologically important oxidizing agent is intermediate between that of *tert*-butyl hydroperoxide and a peracid. The gas-phase reactivity of FlHOOH toward these four nucleophiles is estimated to be 10^7-10^{12} greater than that of *t*-BuO−OH but 10^2-10^6 less than that of peroxyformic acid. The intrinsic gas-phase barriers for the oxidation of $(CH_3)_3N$ and $(CH_3)_2S$ with **3** (FlHOOH) differ by only 1 kcal/mol. The experimentally observed 10^6 rate difference for amine oxidation with protein-bound FlHOOH versus synthetic flavinhydroperoxide (FlEtOOH) in solution is attributed simply to solvent effects; no special activation of the amine by the local enzymatic environment is required for this xenobiotic oxidation. A comparison of estimated O−O bond dissociation energies for CH_3O-OH and CH_3O-OCH_3, at the AM1, Hartree−Fock, B3LYP, CBS-Q, and G3 levels of theory is presented. The performance of AM1, Hartree−Fock, versus CASSCF and QCISD(T) computational methods for the O−O bond elongation in CH_3O-OH and CH_3O-OCH_3 is discussed. Our results provide an estimate of 40 kcal/mol for the O−O bond energy in 4a-flavinhydroperoxide (FlHOOH).

1. Introduction

Flavoprotein monooxygenases are capable of catalyzing a wide variety of oxygen atom transfer reactions. *p*-Hydroxybenzoate hydroxylase (PHBH) is among the most thoroughly studied enzymatic reactions and has become the model for the study of flavoprotein monooxygenases (FMOs).[1] A substantial literature exists for both mechanistic[2−5] and crystallographic[6−9] studies on the PHBH-catalyzed monooxygenation of *p*-hydroxybenzoate (*p*-OHB) to form 3,4-dihydroxybenzoate. The overall oxidative process occurs in two discrete stages. In the initial reductive half-reaction, *p*-OHB and reduced nicotinamide adenine dinucleotide phosphate (NADPH) bind to the enzyme and NADPH reduces the flavin adenine dinucleotide (FAD) cofactor. In the oxidative half-reaction, reduced flavin reacts with oxygen to form C(4a)-flavin hydroperoxide (FlHOOH). Intermediate hydroperoxide **1** is thought to hydroxylate the substrate by transferring its OH group to the 3-position of *p*-OHB.[2−5]

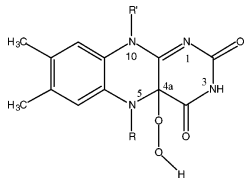

The newly formed 4a-flavinhydroperoxide can either productively hydroxylate the substrate or, in an unproductive mode, it can eliminate HOOH to re-form the oxidized flavin (Fl_{ox}).[10a] The reported half-life for FlHOOH (2.5 ms)[11] is a measure of the facile elimination of HOOH to re-form oxidized flavin and is not related to the thermodynamic stability of the O−O bond in **1**. FlHOOH (**1**) does appear to possess thermodynamic stability when hydrogen-bonded to its surrounding residues.[6b]

Relatively few theoretical studies aimed at the mechanism of PHBH processes have been reported. Vervoort et al.[13] have suggested on the basis of AM1 calculations that a correlation exists between ln k_{cat} for the conversion of a series of 4-benzoate substrates and the energy of their highest occupied molecular orbital (HOMO). Peräkylä and Pakkanen[14] studied the proton-transfer step in the ortho hydroxylation of *p*-OHB. On the basis of HF/3-21G calculations they arrived at the conclusion that the intermediate in the hydroxylation step is the radical OH adduct of *p*-hydroxybenzoate. More recently, Canepa et al.[15] have used density functional theory (DFT) to examine the reactivity of model bicyclic and tricyclic C-(4a)-flavinhydroperoxides (**2** and **3)** relative to other more commonly employed oxidizing agents such as peroxyformic acid in the oxidation of dimethyl sulfide (DMS). Theoretical calculations at the B3LYP/6-31G+(d,p) level suggest that the intrinsic gas-phase reactivity of model C-(4a)-flavinperoxide **3** is about 10^{11} greater than *t*-BuOOH but is about 10^5 less reactive than peroxyformic acid toward DMS.[15]

There have also been several attempts to define the hydroxylation step in PHBH by quantum mechanical/molecular mechanical (QM/MM) methods. Ridder et al.[16] demonstrated a correlation of calculated activation energies with experimental rate constants for an enzyme catalyzed aromatic hydroxylation. Billeter et al.[17] studied the hydroxylation of *p*-hydroxybenzoate in its various anionic states and concluded that the dianion was the most probable form of *p*-OHB at the hydroxylation step.

* Corresponding author.

10.1021/jp035289w CCC: $25.00
Published on Web 10/25/2003

Both of these QM/MM studies used the closed-shell semiempirical AM1 method to study the hydroxylation step that involves O−O bond dissociation.

Closely related flavin-containing monooxygenases (FMOs), where the mechanism is distinctly different from the more commonly studied PHBH enzyme,[18] also fall within this general area of enzymatic oxidation. Kinetic studies, primarily with purified pig liver flavin-containing monooxygenase (FMO1), established that the reduction of dioxygen by NADPH occurs before addition of the xenobiotic substrate. In contrast to PHBH, the presence of the oxygenatable substrate is not required for dioxygen reduction by NADPH. Compounds bearing a soft nucleophilic heteroatom show substrate reactivity provided they come into direct contact with the enzyme-bound 4a-hydroperoxyflavin; FlHOOH is present as the hydroperoxide until a nucleophile makes contact and then it becomes oxidized. Oxidations catalyzed by FMO do not involve substrate−complex equilibrium binding complexes.[18] This requires that the native FlHOOH have a reasonable lifetime at the active site since the reaction of the hydroperoxyflavin form of the enzyme with the xenobiotic substrate (typically an amine or sulfide) is a second-order reaction not saturable by substrate. Consistent with this suggestion, in the absence of the enzymatic environment and in aqueous solution under pulse radiolysis experimental conditions, the breakdown of FlHOOH into Fl_{ox} and HOOH is very rapid ($t_{1/2} = 2.5$ ms).[11]

Conventional wisdom dictates that enzyme protein has little or no effect upon the rates of reaction of 4a-hydroperoxyflavin with compounds bearing sulfur, selenium, or other readily polarizable heteroatoms; nitrogen atoms in amines or hydrazines were presumed to be much less nucleophilic. Jones[19] has presented rate data that the FlHOOH bound to FMO oxidizes amines at least 10^6 times faster than in the absence of enzyme protein. This observation prompted the conclusion[18c] that "how the enzyme increases the nucleophilicity of amines is not known and remains one of the major unsolved facets of the catalytic mechanism of FMOs." We now provide cogent arguments that oxygen transfer reactions with amines have relatively low activation barriers, intrinsically, that require no special participation by the enzyme to "prepare the substrate for oxidation."[18a] We suggest that this is simply a solvent effect and it is the amine oxidation in solution, in the absence of the protein environment, that experiences the rate reduction.[20] In the present study we also examine the level of theory essential to the reasonably accurate estimate of the O−O bond dissociation energy of FlHOOH and the mechanism for the oxidation of a series of xenobiotic nucleophiles.

2. Computational Details

Quantum chemistry calculations were carried out by use of the Gaussian98 program system[21] utilizing gradient geometry optimization.[22] All geometries were fully optimized by use of the B3LYP functional[23,24] with 6-31G(d) and 6-31+G(d,p) basis sets. Vibrational frequency calculations at the same level of geometry optimization were performed to characterize the stationary points as either minima or transition structures (first-order saddle point). Frequency calculations for the larger tricyclic systems were at 6-31G(d). Bond dissociation energies (BDE) at the G2 level are presumed to be within 1−2 kcal/mol of experimental values. The G2 theory[21b] uses fourth-order Møller−Plesset calculations along with various large basis sets up to 6-311G(2df,p). The complete basis set extrapolation method (CBS-Q)[21c] provides energetics equal to or slightly better than G2 theory over the same test set of experimental data. Zero-point energies (ZPE) and thermal corrections to obtain reaction enthalpies at 298 K in the G2 series are by convention computed at the HF/6-31G(d) level and those at the B3LYP/6-31G(d) level were scaled by 0.9806. *Relative* proton affinities (PA) were estimated as the difference in total energy between the protonated and the corresponding neutral species by use of single-point energy corrections [B3LYP/6-31+G(3df,2p)] on a 6-31+G-(d,p) geometry (with the exception of the larger systems). Unless specified to the contrary, all classical energy barriers ($\Delta E^{\ddagger}$) quoted in the text are at the B3LYP/6-31+G(d,p) level and are given without ZPE corrections. A comparison of barrier heights with 6-31+G(d,p) and 6-31+G(3df,2p) basis sets is given in Table 3. Barrier heights reported herein for oxidation by FlHOOH are computed relative to isolated reactants, e.g., trimethylamine and the oxygen atom donor. Barriers calculated from a prereaction complex are typically higher as a result of a lowering of the energy of the reactants due to hydrogen bonding or complexation. A comparison of such oxidation barriers with those calculated from a prereaction complex involving *tert*-butyl hydroperoxide is given in Table 2. Corrections for solvation were made by use of polarizable conductor COSMO model calculations.[21d]

3. Results and Discussion

3.1. Theoretical Treatment of O−O Bond Cleavage. Computational studies of enzyme reactions have recently been greatly assisted by the advent of such quantum mechanical methods as QM/MM and quantum mechanical−free energy (QM−FE) methodologies.[25] Such semiempirical methods offer the distinct advantage of treating the active-site residues within a QM framework, as well as the surrounding protein environment by molecular mechanic or force field methods. However, caution should be exercised with certain types of enzymatic transformations to ensure that the principal chemical event under study is adequately treated by such semiempirical methods. The recent disclosure of several QM/MM studies on *p*-hydroxybenzoate hydroxylase (PHBH), where the oxygen transfer step from 4a-flavin hydroperoxide to *p*-hydroxybenzoate was treated at the AM1 level, is a case in point.[16,17]

During the past decade, we have proffered many times that such reactions, where the key oxygen atom transfer involved oxygen−oxygen bond rupture in the rate-limiting step, require electron-correlated levels of theory in order to adequately describe the energetics of O−O bond cleavage.[26] For example, the O−O bond dissociation energy (BDE) of peroxyformic acid at the Hartree−Fock level is only about 1 kcal/mol.[26a] Therefore, as we examine the nature of the oxygen atom transfer from a fairly realistic model 4a-flavin hydroperoxide **3**, we also examine the level of theory required to reliably treat this specific oxygen transfer step.

The O−O BDEs of CH_3O−OH ($\Delta H_{298} = 44.6$ kcal/mol) and *t*-BuO−OH ($D_\circ = 45$ kcal/mol) are reasonably well established.[27,28a] Recently, on the basis of pulse radiolysis experiments, the O−O BDE of FlHOOH has been suggested to be less than 26 kcal/mol.[29] If the O−O BDE of FlHOOH is actually that low, then the thermodynamic stability of the hydroperoxide comes into question and chemistry derived from homolytic O−O bond dissociation should be anticipated with the formation of hydroxyl radicals. If a simple S_N2-like displacement on the distal oxygen of FlHOOH is operational, as these theoretical data suggest,[15] then the influence of such a low O−O bond dissociation energy (BDE) should be addressed.

Highly accurate O−O BDEs with systems having 10 heavy atoms or less can be calculated at the G2, G3, and CBS-Q levels

TABLE 1: O−O Bond Dissociation Energies and Homolytic Bond Energies Calculated at the AM1, HF, and B3LYP Levels of Theory

	AM1		HF/6-31G(d)		B3LYP/6-31+G(d,p)	
	ΔE^a	$\Delta H_{298}{}^b$	ΔE^a	$\Delta H_{298}{}^b$	ΔE^a	$\Delta H_{298}{}^b$
MeOOH	22.8	17.5	−4.0	−9.2	42.3	37.5 (44.7)[c]
MeOOMe	8.5	3.1	−8.0	−13.2	34.2	28.7 (38.5)[c]
t-BuOOH					41.5	36.7[d] (45.0)[e]
tricyclic FlHOOH	26.7	21.8	−2.7	−7.2	36.7	32.7[d]

[a] O−O homolytic bond energies (ΔE) are given in kilocalories. [b] O−O bond dissociation energies (BDEs; ΔH_{298}) are given in kilocalories per mole. [c] O−O BDE value calculated at CBS-Q level of theory. [d] Thermal corrections for H_{298} are calculated at the B3LYP/6-31G(d) level and are scaled by factor = 0.9804. Other enthalpies are taken directly from the outputs of frequency calculations. [e] O−O BDE value calculated at the G3 level of theory.

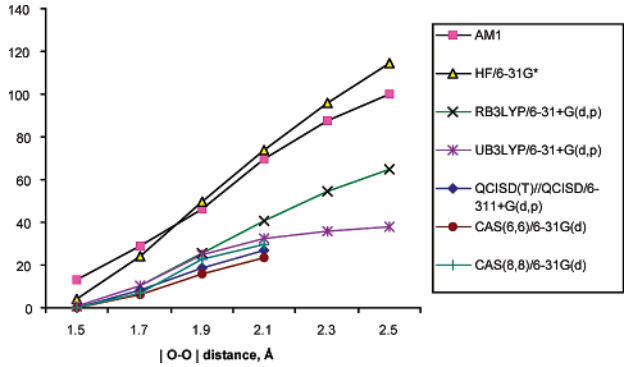

Figure 1. Relative energy of CH_3OOH vs O−O bond elongation calculated with respect to the energy of the equilibrium ground-state geometry at different levels of theory.

of theory.[27] For example the O−O BDE (bond dissociation enthalpies at 298 K) for HO−OH, CH_3O−OH, and CH_3O−OCH_3 at the CBS-Q level are 50.7, 44.7, and 38.5 kcal/mol (experimental values are 50.5, 44.6, and 37.8 kcal/mol).[27] The BDEs for CH_3O−OH at the B3LYP/6-31+G(d,p), AM1, and HF/6-31G* levels are 37.5, 17.5, and −9.2 kcal/mol, suggesting much better treatment of the homolytic O−O bond dissociation for these simple peroxides by the DFT method. The BDE (ΔH_{298}) for homolytic O−O bond rupture for CH_3O−OCH_3 at the AM1 (3.1 kcal/mol) and HF/6-31G(d) [−13.2 kcal/mol] are also inadequate, whereas B3LYP/6-31+G(d,p) produces the more acceptable value of 28.7 kcal/mol (Table 1).

The energy required for homolytic O−O bond dissociation is not necessarily a good measure of the energy of heterolytic O−O bond cleavage attending oxygen atom transfer. The transition structures in QM/MM studies of the potential energy surface (PES) are typically *approximated* by successive elongation of the O−O bond (and formation of the developing C−O bond). To test the validity of this approximation we have examined the energetics of O−O bond elongation in a similar fashion. In a related study on phenol hydroxylase, methyl hydroperoxide was used as a model oxidant in an effort to test the validity of the AM1 wave function in oxygen transfer to the phenoxy anion.[17] We did energy scans for O−O bond cleavage for CH_3O−OH at the RAM1, RHF/6-31G(d), RB3LYP/6-31+G(d,p), UB3LYP/6-31+G(d,p), QCISD(T)//QCISD/6-311+G(d,p), CASSCF(4,4)/6-31G(d), and CASSCF(6,6)/6-31G(d) levels (Figure 1). The O−O bond lengths at equilibrium were calculated by these seven methods to be 1.29, 1.40, 1.46, 1.46, 1.45, 1.49, and 1.48 Å. When the O−O bond in CH_3O−OH had been elongated from 1.5 to 2.1 Å in steps of 0.2 Å (a typical O−O bond distance in a TS is ≈2 Å), in each case, increases in energy of 56.5, 70.0, 40.6, 32.1, 26.8, 23.3, and

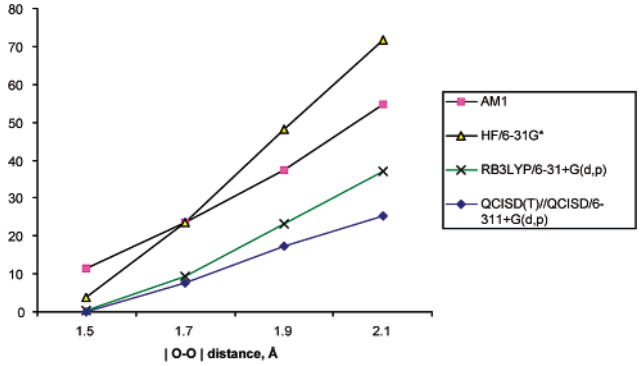

Figure 2. Relative energy of CH_3O−OCH_3 vs O−O bond elongation calculated with respect to the energy of the equilibrium ground-state geometry at different levels of theory.

29.8 kcal/mol resulted [without CASSCF(MP2) corrections; active orbitals are given in Supporting Information].

Energy scans for dimethyl peroxide at RAM1, RHF/6-31G(d), RB3LYP/6-31+G(d,p), and QCISD(T)//QCISD/6-311+G(d,p) levels (Figure 2), where the initial minimum O−O bond distances were 1.29, 1.40, 1.46, and 1.45 Å, evidenced energy increases of 43.4, 67.8, 36.7, and 25.2 kcal/mol at an O−O distance of 2.1 Å.

The plots in Figures 1 and 2 show that AM1 and HF/6-31G(d) methods overestimate the energy of O−O bond elongation by as much as 100% when compared with our higher-level QCISD(T) and CASSCF calculations, whereas UB3LYP/6-31+G(d,p) shows the best agreement with the more rigorous methods. Nevertheless, the UB3LYP/6-31+G(d,p) method does overestimate the O−O bond elongation energy by about 5 kcal/mol at an O−O distance of 2.1 Å [32.5 vs 27.0 kcal/mol with the QCISD(T) and UB3LYP methods]. Significantly, Figure 1 demonstrates that restricted B3LYP/6-31+G(d,p) produces similar results to unrestricted UB3LYP/6-31+G(d,p) calculations on O−O bond elongation up to 1.9 Å. Since the O−O bond distance in most TSs is typically 2.0 Å or less, transition structure geometry optimizations are generally acceptable at the RB3LYP/6-31+G(d,p) level of theory. This is quite fortunate since calculations at the unrestricted level nearly double the computational time required. The energy required for homolytic bond cleavage of the O−O bond in model FLHOOH **3** with the AM1 and RB3LYP/6-31+G(d,p) wave functions is 21.8 and 32.7 kcal/mol (Table 1). As noted above the experimental estimate for the O−O BDE in FlHOOH **1** is <26 kcal/mol[29] while for tertiary hydroperoxide, *t*-BuO−OH, both the calculated (45.0 kcal/mol, G3)[21] and experimental BDEs (44.1 kcal/mol, and $D_\circ$ = 45 kcal/mol)[28a] are appreciably higher. At the B3LYP/6-31+G(d,p) level, with B3LYP/6-31G(d) thermal corrections for the enthalpy, the BDE for O−O bond in *t*-BuO−OH is estimated to be 36.7 kcal/mol. Since BDEs derived from the B3LYP calculations underestimate the O−O bond energies by 6−8 kcal/mol, we estimate the O−O BDE in model peroxide **3** to be ≈40 kcal/mol. Since the N5 alkylated flavin hydroperoxide **1b** (FlEtOOH)[30] is sufficiently stable to be isolated and characterized, it is likely that the experimental estimate[29] for the O−O BDE in FlHOOH **1** (<26 kcal/mol) is too low.

An energy scan of model FlHOOH **3** shows an energy increase of 72.5 kcal/mol upon O−O bond elongation from 1.3 to 2.1 Å at the RAM1 level (at the UAM1 level the increase was only 24.3 kcal/mol based upon the same O−O bond elongation). Thus, this entire series of peroxides exhibits very poor agreement with experiment for the O−O bond energies and distances at the AM1 level, and a potential energy surface

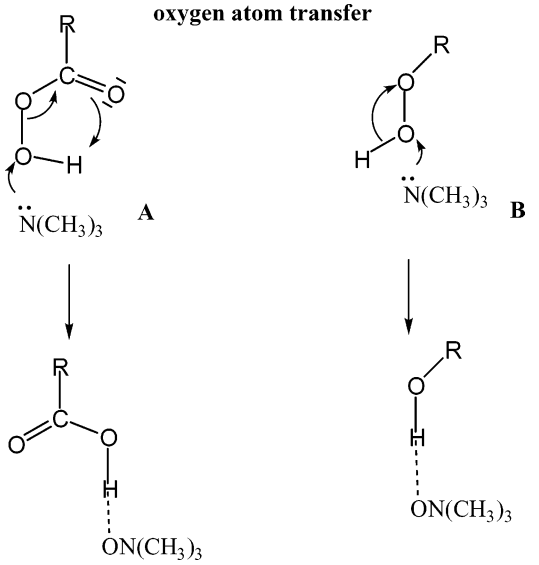

Figure 3. Mechanistic pathway for oxygen atom transfer from peroxyformic acid (A) and alkyl hydroperoxides (B) to trimethylamine.

involving oxygen transfer from flavinhydroperoxide with this method should have a highly exaggerated barrier height. Despite these apparent shortcomings, the estimated AM1 activation energy for the hydroxylation step was 17.6 kcal/mol;[16b] the experimental activation energy has been estimated to be around 12 kcal/mol.[31] This calculated activation barrier was obviously not addressing specifically the energetics of O−O bond cleavage.

Density functional theory, especially the B3LYP variant, has been used successfully in a variety of oxidative procedures involving O−O cleavage and affords activation barriers in good agreement with experiment.[26] For example, the calculated activation barrier for the *m*-chloroperoxybenzoic acid epoxidation of cyclohexene agrees within 1 kcal/mol with the experimental value.[26f] DFT has also been used to calculate the O−O BDE in a series of fluoro-substituted peroxides.[28b] We now apply this methodology to the optimization of transition structures, modeling oxygen transfer from 4a-flavin hydroperoxide **3** to trimethylamine, dimethyl sulfide, dimethylselenide, and trimethylphospine. We also describe a unique method to distinguish between an oxygen atom transfer and hydroxyl transfer in this series of nucleophiles.

3.2. Electronic Factors Influencing Oxygen Atom versus Hydroxyl Transfer. The rate of heterolytic O−O bond cleavage in oxygen atom transfer reactions is a function of the stability of the oxyanion leaving group. For example, the O−O bond cleavage in a peracid [R(C═O)O−OH] gives a fairly stable carboxylate anion ($pK_a \approx 5$), while an alkyl hydroperoxide affords an relatively unstable alkoxide ion ($pK_a \approx 16-19$). Oxygen atom transfer from the −OOH moiety can proceed by two basic pathways: (a) the formal transfer of the hydroxyl group followed by an intramolecular hydrogen transfer along the reaction coordinate or (b) a hydroxylation process where the intact OH group is transferred and the leaving alkoxide exists as a minimum connected to the TS. The former is best exemplified by the peracid epoxidation of an amine (Figure 3A) that proceeds by the formal transfer of an essentially neutral OH group to the nitrogen atom of the amine followed by a 1,4-proton transfer to the carbonyl oxygen of the departing carboxylate leaving group *after the barrier is crossed*.[32]

In a similar fashion, the epoxidation of a simple alkene is attended by the cleavage of a relatively weak peracid O−O bond (48.4 kcal/mol)[27a] and the formation of an epoxide and a neutral carboxylic acid. The energetics of reaction are quite favorable with a typical ΔH_{298} of epoxidation on the order of 48−59 kcal/mol.[26f]

The oxidation of a heteroatom bearing a lone pair of electrons (e.g., amine, sulfide, or phoshine) with increased nucleophilicity of the heteroatom typically results in an early TS, especially with phosphines. Since the N−O bond in an N-oxide is particularly weak, this can sometimes be an endothermic reaction,[20] in contrast to the highly exothermic oxidation of a phosphine with its associated very strong P−O bond. Oxygen atom transfer from an alkyl hydroperoxide, however, has additional energy requirements. Since this is typically a heterolytic O−O bond cleavage, the instability of the developing anionic alkoxide can influence the reaction pathway. Thus, the heterolytic cleavage of the O−O bond in *t*-BuOOH affords the relatively poor *t*-butoxide leaving group (pK_a 19). Consequently, the S_N2-like attack on the distal oxygen by a nucleophile such as an amine is attended by a 1,2-proton transfer (Figure 3B) to the departing alcoholate in order to produce neutral *tert*-butyl alcohol and the N-oxide product. The activation barrier for oxygen atom transfer from a hydroperoxide is also controlled, to a very large extent, by the energetics of this 1,2-hydrogen transfer step. Such concerted 1,2-hydrogen transfer reactions to an adjacent lone pair are four-electron processes and as such are formally forbidden.[26b] For example, the 1,2-hydrogen shift in *t*-BuOOH to form the high-energy *tert*-butyl alcohol oxide intermediate (Eq 1) has an activation barrier of 49.5 kcal/mol. This highly endothermic reaction (ΔE = 40.1 kcal/mol) has a very late TS as evidenced by the short O−H bond to the proximal oxygen.

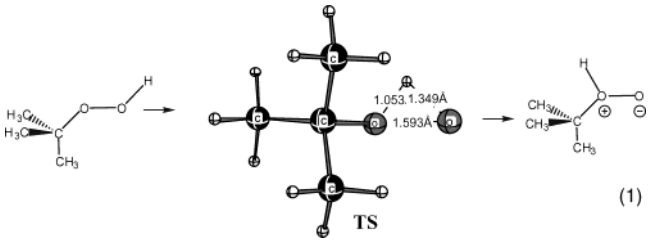

Fortunately, we can discern something about the extent of hydrogen migration in the overall reaction by examining the magnitude of the single imaginary frequency for the TS. When the reaction vector is composed mostly of light-atom hydrogen migration, as in eq 1, the imaginary frequency is quite high at $\nu_i = -1233$ cm^{-1}. Contrariwise, when the reaction vector consists mainly of heavy-atom OH motion as in peracid alkene epoxidation,[32] the single negative imaginary frequency of the first-order saddle point is only about −300 to −450 cm^{-1} (see Table 2 for a summary).

In the middle of these two reaction types is the oxidation of trimethyamine by *t*-BuOOH. The classical gas-phase activation barrier ($\Delta E^{\ddagger}$) from isolated reactants is 30.5 kcal/mol while $\Delta E^{\ddagger}$ =40.8 kcal/mol relative to a prereaction complex ($\Delta G^{\ddagger} = 39.3$ kcal/mol, $\Delta S^{\ddagger} = -4.1$ eu), reflecting the GS stabilization due to hydrogen bonding of the *tert*-butyl hydroperoxide to the basic amine (B3LYP/6-31G(d)). A solvent correction with the COSMO solvation model lowers the classical barrier slightly to 36.4 kcal/mol (solvent = tetrahydrofuran, THF). This TS has a relatively large component of 1,2-hydrogen transfer to stabilize the departing *t*-BuO$^-$ and its imaginary frequency is $\nu_i = -800$ cm^{-1}. Animation of the vectors of this TS shows very little motion of the heavier oxygen atom while the hydrogen atom of the OH is moving rapidly between the two peroxo oxygens in a "windshield wiper motion" (Figure 4A). Consistent with this suggestion the calculated kinetic isotope effect (see Sup-

TABLE 2: Reaction Barriers Calculated with Respect to the Isolated Oxidizing Agent and Substrate[a]

substrate	oxidizing agent	ΔE‡, kcal/mol	imag freq, cm^{-1}
ethylene	H(C=O)OOH	14.1; **14.9**	−448.0
	bicyclic FlHOOH	24.0; **24.1**	−392.3
E2-butene	H(C=O)OOH	10.5; **11.0**	−411.1
	t-BuOOH	32.2; **32.2**	−438.0
	bicyclic FlHOOH	19.9; **19.8**	−408.6
$(CH_3)_3N$	H(C=O)OOH	3.3; **3.0**	−283.2
	t-BuOOH	30.5; **29.0** (40.9)	−800.4
	bicyclic FlHOOH	9.2	
	tricyclic FlHOOH (TS-**5a**)[b]	14.6; **13.8**	−397.0
	tricyclic FlHOOH (TS-**5b**)[b]	12.2;**12.3**	−312.8
	H(C=O)OOH	5.6; **3.7**	−303.0
$(CH_3)_2S$	MeOOH	**27.1** (**32.4**)	−697.9[c]
	MeOOH··· MeOOH (dimer)	10.8; **10.5** (22.5; **19.4**)	−283.8[c]
	t-BuOOH	30.0; **27.2** (36.5; **32.2**)	−672.5
	bicyclic FlHOOH	10.4	−258.5
	tricyclic FlHOOH (TS-**7a**)[d]	14.3; **11.4**	−267.6
	tricyclic FlHOOH (TS-**7b**)[d]	14.1; **12.7**	−286.4
$(CH_3)_2Se$	H(C=O)OOH[e]	−3.7; **−6.5**	−248.1
	t-BuOOH[e]	12.1	−535.9
	tricyclic FlHOOH (TS-**8**)[e]	2.6; **−3.2**	−206.4
	H(C=O)OOH	−0.2; **−0.3**	−280.5
	t-BuOOH	15.3; **14.0** (20.7)	−358.4
$(CH_3)_3P$	tricyclic FlHOOH (TS-**6a**)[b]	3.9; **4.4**	−327.0
	tricyclic FlHOOH (TS-**6b**)[b]	3.9; **5.0**	−338.8

[a] Numbers in parentheses are barriers calculated with respect to the prereaction complex. Classical activation energies (ΔE‡) at the B3LYP/6-31G(d) level are given in lightface type; numbers shown in boldface type correspond to B3LYP/6-31+G(d,p) calculations. The single imaginary frequency of the transition structures was calculated at B3LYP/6-31G(d). [b] Transition structures are shown in Figure 7. [c] The single imaginary frequency was calculated at B3LYP/6-31+G(d,p) level. [d] Transition structures are shown in Figure 9. [e] Transition structures are shown in Figure 10.

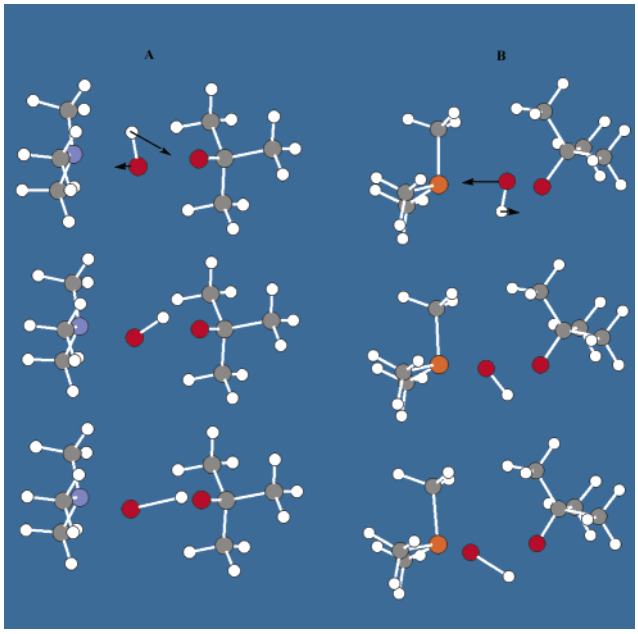

Figure 4. Graphical visualizations of the single imaginary frequencies (B3LYP/6-31G(d)) for the transition structures for oxidation of trimethylamine ($\nu_i = -800.4$ cm^{-1}) and trimethylphosphine ($\nu_i = -358.4$ cm^{-1}) with *t*-BuOOH showing in A three snapshots of the 1,2-hydrogen migration versus initial hydroxyl transfer in path B with proton transfer to the *t*-BuO^- late on the reaction coordinate.

porting Information) for the hydroxyl proton is relatively large with $k_H/k_D = 1.79$ at 298 K.

The oxidation of phosphorus is typically a highly exothermic reaction and consequently has an early TS. The oxidation of trimethylphosphine with *t*-BuOOH has a classical activation barrier of 15.3 kcal/mol relative to isolated reactants while $\Delta E^‡ = 20.7$ kcal/mol relative to a prereaction complex ($\Delta G^‡ = 21.2$ kcal/mol, $\Delta S^‡ = -8.2$ eu) reflecting the more weakly basic phosphine (B3LYP/6-31G(d)). A solvent correction with the COSMO solvation model lowers the classical barrier slightly to 18.8 kcal/mol (solvent = THF). In this case the reaction coordinate involves mostly movement of the heavier OH group. In the oxidation of a phosphine, the hydrogen atom remains relatively still and the heavier oxygen atom swings in a pendulumlike motion between the proximal oxygen and the attacking nucleophilic phosphorus atom (Figure 4B); the hydrogen is transferred after the barrier is crossed. In this type of oxidative procedure, hydrogen migration is not part of the reaction vector and the imaginary frequency is relatively low at $\nu_i = -358$ cm^{-1}, reflecting the greater mass of the transferring oxygen atom. The calculated KIE is reduced accordingly to $k_H/k_D = 1.20$. Thus, the magnitude of the single imaginary frequency of the TS provides information about the nature of the oxygen atom transfer step. For example, in Table 2, the TSs that have relatively basic alkoxide leaving groups such as *t*-BuO^- and CH_3O^- require some form of stabilization of the developing alkoxide and have relatively large imaginary frequencies.

A particularly poignant example of the relevance of the magnitude of the imaginary frequency is exemplified in the oxidation of dimethyl sulfide by CH_3OOH. In a seminal experiment, Edwards and co-workers[33] showed that in aprotic solvent sulfide oxidation is second-order in hydroperoxide and the second molecule of ROOH plays the role of a protic solvent catalyst. The calculated activation barrier for the oxidation of DMS by monomeric CH_3OOH is 32.4 kcal/mol relative to its prereaction complex (Table 2) as a consequence of the relatively poor methoxide leaving group. We observe a marked reduction in activation barrier for the oxidation of DMS when the dimer of CH_3OOH is employed ($\Delta\Delta E^‡ = 13$ kcal/mol). More importantly, there is a change in mechanism that becomes immediately obvious upon examination of the imaginary frequencies of the two TSs. The TS for oxygen atom transfer from monomeric CH_3OOH to DMS has a large degree of hydrogen atom motion involving a 1,2-hydrogen shift and resembles the pathway for oxidation by *t*-BuOOH shown in Figure 4A. The marked reduction in the imaginary frequency from $\nu_i = -698$ to 284 cm^{-1} for the dimeric CH_3OOH oxidation is consistent with very little displacement of the hydrogen atom during vibration of the imaginary frequency as visualized graphically in Figure 5. Upon S_N2 displacement on the distal oxygen, the *hydroxyl group* migrates from the peroxide to the sulfur atom and the developing methoxide anion leaving group is stabilized by hydrogen bonding with the OOH moiety of the *second* CH_3OOH. We see a fairly large component of an H-bonding interaction in the TS *but no component of a 1,2-hydrogen shift* and hence the relatively low imaginary frequency. The hydrogen is transferred from the hydroxyl group of CH_3OOH to the CH_3O^- *after the barrier is crossed.* The energy requirements for the stabilizing influence of the 1,2-hydrogen shift are ameliorated in part by an intramolecular H-bond and hence the activation energy is lowered accordingly. Thus, DMS oxidation by dimeric CH_3OOH is formally a hydroxylation reaction even though formation of the thermodynamic $(CH_3)_sSO$ product does not involve a 1,2-hydrogen shift but rather involves a proton transfer to CH_3OO^- late on the reaction coordinate.

3.3. Oxidation of Amines, Sulfides, Phosphines, and Selenides with C-(4a)-Flavinhydroperoxide. Bruice and co-workers[30] have studied the reactions of a model C-(4a)-

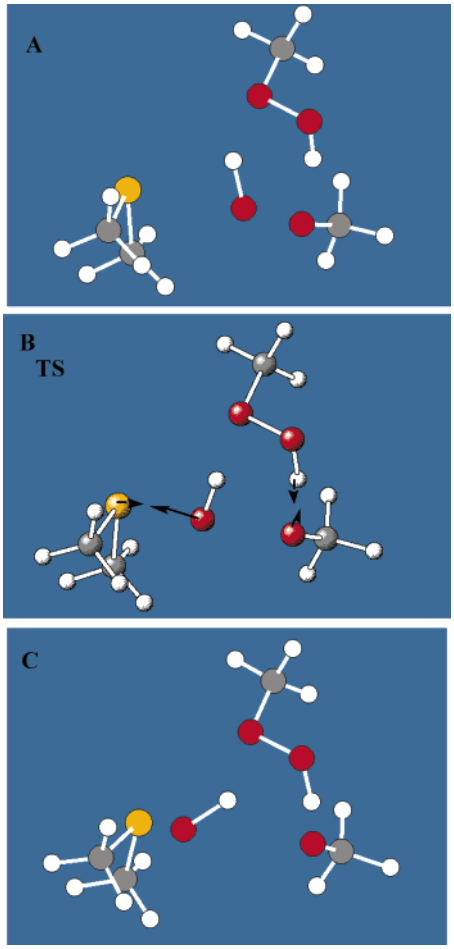

Figure 5. Graphical visualization of the imaginary vibration (ν_i = −283.8 cm^{-1}) characterizing the transition structure (B) for the oxidation of DMS with MeOOH dimer. Structures A and C correspond to the extreme points of the vibration. The TS structure optimization and frequency calculation are at the B3LYP/6-31+G(d,p) level.

hydroperoxide (**1c**) in water-free solvents and found it quite capable of carrying out monooxidation and dioxygenation reactions, quite analogous to certain flavoproteins. When the N5 nitrogen of C-(4a)-hydroperoxide (**1a**) is alkylated with an ethyl group, this FlEtOOH model hydroperoxide can be isolated in the laboratory since this prevents the elimination of C_2H_5-OOH to re-form the oxidized flavin. The N5-ethyl derivative **1b** has been reacted with amines, sulfides, alkenes, and I^-, and its reactivity has been compared to such common oxidants as hydroperoxides and peracids.[30]

In the present study, geometry optimizations were carried out with a relatively flexible basis set [B3LYP/6-31+G(d,p)] that includes the plus basis set that adequately treats anions and the oxygen lone pairs of the O−O bond. Polarization functions were added to the hydrogens to better describe hydrogen-bonding interactions. The use of a larger basis set [6-31+G(3df,2p), Table 3] does not affect the barriers significantly.

Due to the size of a tricyclic 4a-FlHOOH molecule, bicyclic model hydroperoxide **2** was used in some cases. We chose initially several simple model substrates for this comparison that are presented in Tables 2 and 3. To estimate the relative reactivity of bicyclic and tricyclic C4a-hydroperoxyflavin models **2** and **3**, we compared their reactivity to that of the paradigm model theoretical oxygen atom donor, peroxyformic acid [H(C=O)OOH]. The barriers for the epoxidation of ethylene and *E*-2-butene with bicyclic model hydroperoxide **2** are on average 9 kcal/mol greater than for peroxyformic acid

TABLE 3: Reaction Barriers ($\Delta E^{\ddagger}$) and Reaction Energetics (ΔE_{reac}) Calculated with Respect to the Isolated Oxidizing Agent, FlHOOH 3, and Substrate[a]

substrate	$\Delta E^{\ddagger}$, kcal/mol	ΔE_{reac}, kcal/mol
$(CH_3)_3N$	12.3, **13.5** (TS-**5b**)	**−5.3**
$(CH_3)_3P$	5.0, **5.0** (TS-**6b**)	**−90.7**
$(CH_3)_2S$	12.7, **11.8** (TS-**7b**)	**−43.7**
$(CH_3)_2Se$	−3.2 (TS-**8**)	**−38.2**

[a] Lightface type corresponds to B3LYP/6-31+G(d,p) calculations. Energy refinement at the B3LYP/6-31+G(3df,2p)//B3LYP/6-31+G(d,p) level of theory is given in boldface type.

(Table 2). The reactivity of *t*-BuOOH as an oxygen atom donor is much less than that of bicyclic hydroperoxide **2**. Peroxyformic acid is also much more reactive toward DMS than the simplest hydroperoxide, methyl hydroperoxide ($\Delta\Delta E^{\ddagger}$ = 23 kcal/mol). However, CH_3O-OH and *t*-BuO−OH exhibit very similar reactivities toward dimethyl sulfide (DMS).[15] While CH_3OOH and *t*-BuOOH have comparable barriers for the oxidation of DMS, bicyclic model flavin **2** exhibits a much lower activation barrier of only 10.4 kcal/mol ($\Delta\Delta E^{\ddagger}$ = 10 kcal/mol). Thus, bicyclic hydroperoxide **2**, with its three electron-withdrawing substitutents at C4, is a much better oxygen donor than *t*-BuOOH as reflected in the relative stability of the leaving group alcoholates.

Preliminary studies with bicyclic hydroperoxyflavin **2** for the oxidation of trimethylamine (TS-**4**, not shown) show that this oxidation has a classical barrier of only 9.2 kcal/mol (eq 2) at the B3LYP/6-31+G(d,p) level (Table 2). In gas phase, trimethylamine is slightly more nucleophilic with this oxidant than dimethyl sulfide ($\Delta E^{\ddagger}$ = 10.4 kcal/mol).

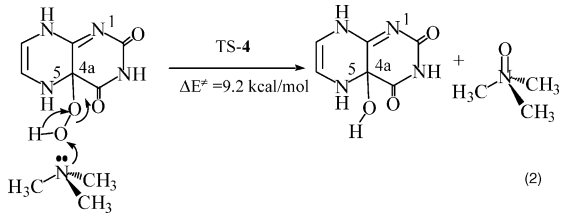

To examine the potential role of the ribityl side chain of the native flavinhydroperoxide, a β-hydroxyethyl group was included to model its 2′-OH group. A dimethylbenzene ring was added to complete the tricyclic hydroperoxide (minimum **3**, Figure 6).

There has been surprisingly little attention paid to a potential catalytic role for the 2′-OH group. X-ray structures,[6−9] on neutral PHBH systems, typically show this hydroxyl group in the plane of the flavin ring and pointed away from the basic N_1 position, and a Leu-299 residue is within hydrogen-bonding distance of N_1 (3.1−3.5 Å between nitrogens). A modest H-bond of the hydroperoxide group to the O4 carbonyl oxygen exists in FlHOOH **3**. The ultimate alcohol product of the oxygen transfer reaction (FlHOH) and the intermediate alcoholate leaving group ($FlHO^-$) are both seriously puckered tricyclic structures,[34] and the latter has a strong H-bond between the 2′-OH group and N_1 (1.89 Å).

The oxidation of trimethylamine by tricyclic hydroperoxide **3**, surprisingly, exhibits a higher activation barrier ($\Delta\Delta E^{\ddagger}$ = 4.6 kcal/mol) than bicyclic hydroperoxide **2** (eq 3). The transition structure for oxygen-atom transfer from model C4a-hydroperoxyflavin **3** to Me3N (TS-**5a**, Figure 7) exhibits an imaginary frequency of −397 cm^{-1} and the TS is composed largely of hydroxyl transfer with proton transfer to the departing $FlHO^-$ coming after the barrier is crossed.

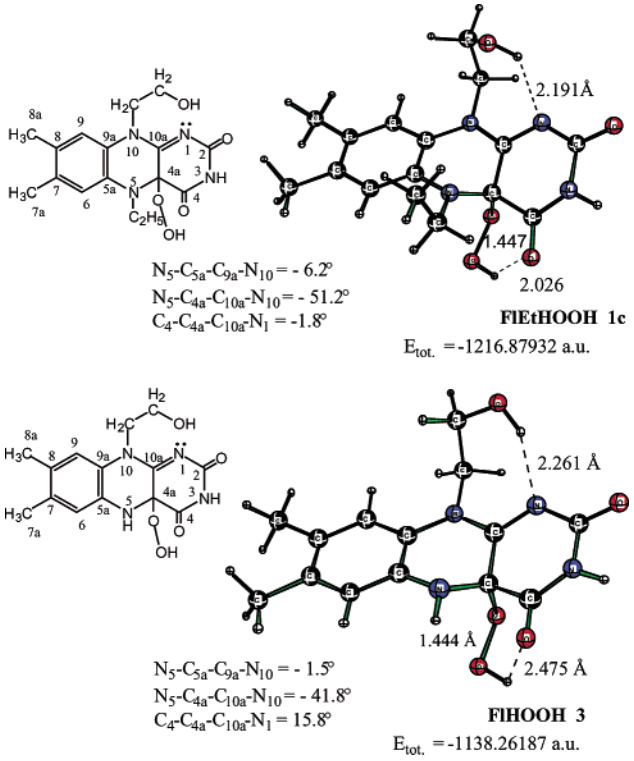

Figure 6. B3LYP/6-31+G(d,p) optimized structures of FlEtOOH **1c** and FlHOOH **3**.

We also located a second TS for the oxidation of Me_3N (TS-**5b**, Figure 7) that involved H-bonding of the OOH group to the O-4 carbonyl oxygen. This intramolecular H-bond reduces the 1,2-hydrogen migration component with an attending decrease in the imaginary frequency to -313 cm^{-1} and lowers the barrier by 1.5 kcal/mol. Three snapshots of the animation of the vibration of the single imaginary frequency shown in Figure 8 demonstrate an almost indistinguishable displacement of the OH *hydrogen atom* at the extreme positions of the oxygen atoms during its vibration.

We also corroborate the earlier suggestion by Bruice and coworkers[30] that the N-oxidation of tertiary amines by the *N*5-ethyl derivative of lumoflavin (**1a)** involved nucleophilic displacement by sp^3-hybridized nitrogen on the terminal oxygen of the hydroperoxide (eq 3). We carried out the gas-phase oxidation of trimethylamine using the *N*-ethyl derivative of **3** (**1c**). The activation barrier for formation of the N-oxide of Me_3N by oxygen atom transfer from hydroperoxide **1c** (TS-**5c**,

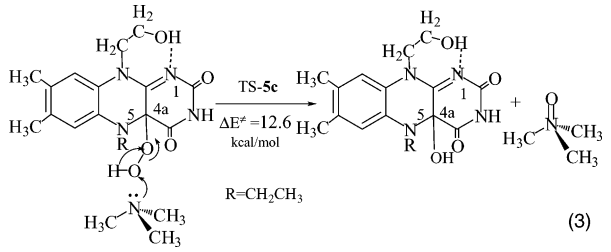

(3)

Figure 7**)** has an activation barrier (12.6 kcal/mol) only slightly higher than that calculated for TS-**5b**. Thus, the presence of the *N*5-ethyl substituent has essentially no impact upon the overall rate of N-oxidation. It was further established that the efficiency of 4a-FlEtOOH **1b** in N-oxidation in solution[30] was more than 4 orders of magnitude greater than that of H_2O_2 or *t*-BuOOH. Contrariwise, *m*-chloroperbenzoic acid was found to be ca. 10^5 times more reactive than 4a-FlEtOOH.[30] The correlation of the pK_a of the departing "alcohol" for a series of ROOH oxygen donors led to the suggestion that the increased reactivity of C4a-hydroperoxyflavin can be attributed to the inductive stabilization of the alcoholate leaving group by the electronegative elements surrounding C4. The experimentally estimated pK_a of 4a-FlEtOOH is 9.4, while the pK_a of *t*-BuOH is approximately twice that. We estimate the *relative* proton affinity of the C4a-hydroxyflavin (FLHOH) derived from oxygen transfer from **3** to be 339 kcal/mol [B3LYP/6-31+G(d,p)] while that of *t*-BuOH is much greater at 381 kcal/mol [B3LYP/6-31+G(d,p)]. In the oxygen transfer step, the developing oxyanion of **3** ($FlHO^-$) is much better stabilized as the O−O bond is cleaved than is *t*-butoxy anion, and this is clearly reflected in their difference in activation energies for the oxidation of Me_3N ($\Delta\Delta E^{\ddagger}$ = 16.7 kcal/mol, Table 2). Thus, extension of model hydroperoxide **2** to include the *o*-dimethylbenzene ring and the intramolecular hydrogen-bonded "ribityl side chain" has only a minor impact upon the activation barrier for oxygen-atom transfer to DMS[15] ($\Delta\Delta E^{\ddagger}$ = 1.0 kcal/mol, Table 1) but a somewhat larger barrier difference for Me_3N ($\Delta\Delta E^{\ddagger}$ = 3.1 kcal/mol). As noted above, the 2′-OH group does have a stabilizing influence on the developing alcoholate ($FlHO^-$).

We also examine more closely the relative reactivity of sulfur versus nitrogen as the nucleophile in this series (Figure 9). Oxygen atom transfer from tricyclic model C4a-hydroperoxyflavin **3** to DMS (TS-**7a**, $\Delta E^{\ddagger}$ = 11.4 kcal/mol)[15] exhibits a slightly lower activation barrier at the B3LYP/6-31+G(d,p) level than trimethylamine ($\Delta E^{\ddagger}$ = 12.3 kcal/mol).[14] The intrinsic gas-phase reactivity of Me_2S is less than an order of magnitude greater than that of Me_3N for oxidation with hydroperoxyflavin **3** ($\Delta\Delta E^{\ddagger}$ = 0.9 kcal/mol). In the initially reported TS for Me_2S oxidation,[15] the hydroperoxide hydrogen is migrating to the proximal oxygen in much the same way as that in trimethylamine TS-**5a**, and the methyl groups of DMS are anti to the O−H bond. The modest lowering of the activation barrier ($\Delta\Delta E^{\ddagger}$ = 1.5 kcal/mol) by such an intramolecular H-bond in TS-**5b** prompted a closer look at related reactions.

The range of xenobiotics accepted by the pig liver enzyme includes inorganic as well as organic compounds with some of the better substrates containing sulfur or selenium instead of nitrogen.[18] Structure−reactivity relationships suggest that, in addition to nucleophilicity, size and charge are also important parameters that may limit access to the enzyme-bound FlHOOH. Since the hydroperoxide is formed prior to arrival of the xenobiotic substrate, oxidation occurs on the very first step in this catalytic cycle.[18] The elimination of water from FlHOH in the next step to re-form the oxidized flavin (Fl_{ox}^-) is 10 times slower than any of the other steps. Hence, the release of water is rate-limiting and is responsible for the observation that V_{max} is essentially the same for all substrates.[35] From the size and shape of acceptable substrates it has been surmised that the FlHOOH in human FMO1 lies at the bottom of a cleft no more than 4.5 Å in diameter and about 5 Å below the surface of the amino acid side chains that control access to the oxidizing agent. These observations pose an additional problem for the orientation that a disulfide or diselenide must have in order to be effectively oxidized within the confines of the relatively small cavity. Consequently, we have examined carefully the approach of these dialkyl nucleophiles to FlHOOH **3**.

We located a second TS for DMS oxidation (TS-**7b**, Figure 9) that incorporated both the intramolecular H-bond to O4 and the methyl groups rotated in such a way that they are in an anti-staggered conformation with the O−H bond of the distal oxygen in the TS. Surprisingly, when the hydroperoxide hydro-

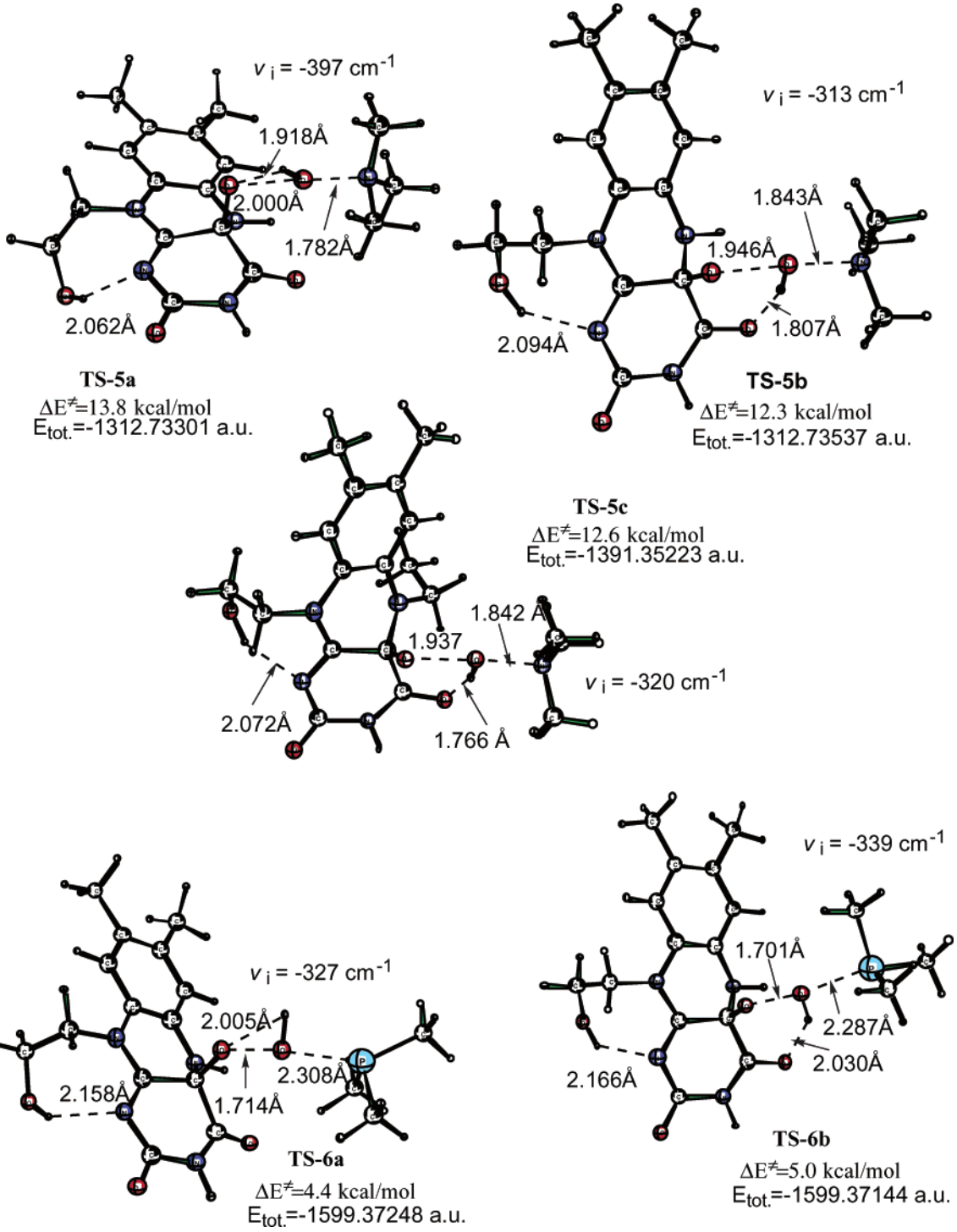

Figure 7. Transition structures for the oxidation of $(CH_3)_3N$ and $(CH_3)_3P$ with tricyclic FlHOOH **3** and **1c** optimized at the B3LYP/6-31+G(d,p) level of theory. Imaginary frequencies are at the B3LYP/6-31G(d) level.

gen is H-bonding to O4 as shown in the TS-**7b** (Figure 9), the barrier is slightly increased to 12.7 kcal/mol. The methyl groups are oriented down and away from the peroxo moiety with the smaller 6-31G(d) basis set but when diffuse and polarization functions are added [6-31+G(d,p)], rotation about the O−S bond axis ensues and the opposite orientation of the methyl groups results (TS-**7b**). The barrier showed virtually no change and both TSs were higher in energy ($\Delta\Delta E^{\ddagger} = 1.3$ kcal/mol) than TS-**7a** in the absence of this H-bonding "stabilizing" influence.

We also examined the effect of the orientation of the methyl groups with respect to the oxidation of dimethylselenide (Figure 10). Geometry optimization of TS-**8** (Figure 10) started with the methyl groups down as in TS-**7a** but proceeded to rotate and finally arrive at TS-**8**. The activation barrier for the oxidation of $(CH_3)_2Se$ is quite low (TS-**8**, $\Delta E^{\ddagger} = -3.2$ kcal/mol). The classical barrier for the formation of $(CH3)_2Se-O$ by the action of *t*-BuOOH is considerably higher ($\Delta E^{\ddagger} = 12.1$ kcal/mol, Figure 10) as anticipated for the much weaker oxidizing agent. The wave function for this TS was stable as evidenced by reoptimizing the TS at UB3LYP/6-31+G(d,p) and arriving at the same total energy. Thus, the selenium compound is much more nucleophilic toward **3** than either the sulfur or phosphorus atoms. The Me_2Se barriers for *t*-BuOOH, FlHOOH, and peroxyformic acid are 12.1, −3.2, and −6.5 kcal/mol.

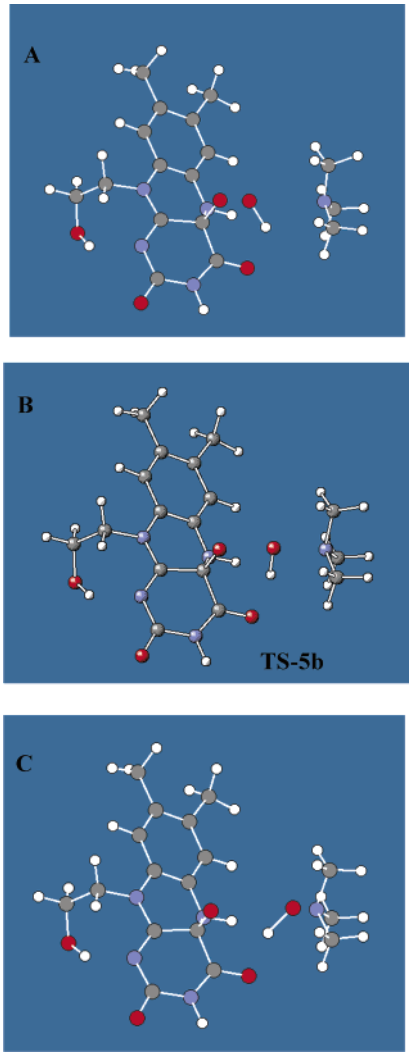

Figure 8. Graphical visualization of the imaginary vibration (ν_i = −312.8 cm^{-1}, B3LYP/6-31G(d)) characterizing the transition structure (B) for the oxidation of Me_3N with FlHOOH **3**. Structures A and C represent structures corresponding to the extreme points of the vibration.

We also observe the same trend for the relative reactivity of sulfur versus selenium as we did with N versus P nucleophiles. The barrier differences for S versus Se with *t*-BuOOH ($\Delta\Delta E^{\ddagger}$ = 15.1 kcal/mol) are narrowed somewhat with FlHOOH ($\Delta\Delta E^{\ddagger}$ = 14.6 kcal/mol) and even further with the more reactive oxidizing agent peroxyformic acid ($\Delta\Delta E^{\ddagger}$ = 10.3 kcal/mol). FMO[19] studies on the oxidation of different substrates by both synthetic (FlEtOOH, **1b**) and enzyme-bound 4a-hydroperoxyflavin (FlHOOH) presented an interesting dichotomy in the relative reactivity of sulfur and nitrogen xenobiotics. The experimental rate data suggested that enzyme protein has surprisingly small effects upon the rate of oxidation of sulfur compounds. However, for nitrogen-containing compounds the rate enhancements of the enzyme over the synthetic protein-free hydroperoxyflavin **1b** was about 6 million-fold. This prompted the suggestion that the protein plays a significant role in the oxidation of nitrogen compounds but participates only marginally in the oxidation of sulfur compounds by the enzyme-bound oxidant. The enzyme-bound flavinhydroperoxide oxidized *N*,*N*-dimethylaniline almost an order of magnitude faster than thiophenol.[18] Alternatively, we find that the intrinsic gas-phase barrier for the oxidation of trimethylamine is about 1 kcal/mol greater than that for dimethyl sulfide. We suggest that solvent effects played a major role in oxidation with the synthetic

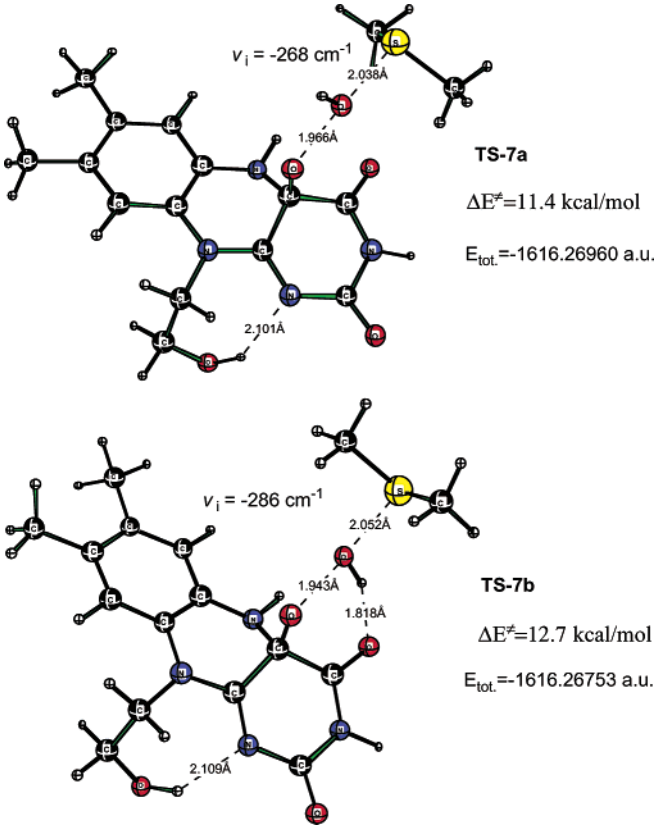

Figure 9. Transition structures for the oxidation of DMS with tricyclic FlHOOH **3** optimized at the B3LYP/6-31+G(d,p) level of theory. The barriers are estimated with respect to isolated reactants. Imaginary frequencies are at the B3LYP/6-31G(d) level.

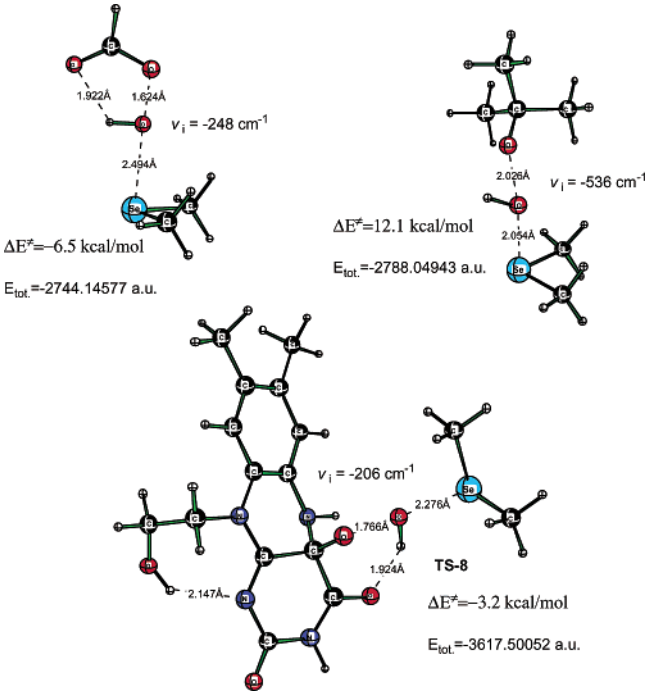

Figure 10. Transition structures for the oxidation of Me_2Se with peroxyformic acid, *t*-BuOOH and tricyclic FlHOOH **3** optimized at the B3LYP/6-31+G(d,p) level of theory. The barriers are estimated with respect to isolated reactants. Imaginary frequencies are at the B3LYP/6-31G(d) level.

flavinhydroperoxide (FlEtOOH) in solution since the nitrogen-containing compounds are much more basic than the sulfur nucleophiles. Examination of the experimental rate data[18b] sug-

gests that it is the rate of amine oxidation that is suppressed in its reaction with the synthetic flavinhydroperoxide **1b,** with far more subtle changes in the rate of sulfur oxidation. If the amine is more highly solvated than the sulfur nucleophile in protic media, then perhaps what was actually measured was the greater degree of ground-state solvation of the amine and how that depresses the rate of amine oxidation. Thus, it is *not the enhancement of the enzyme rate* that was observed but rather it is the *decrease in the protein-free rate* that should be emphasized.

Our predilection to assign phosphorus a much greater nucleophilic capacity than nitrogen or sulfur is based upon nucleophilic constants that were determined in methanol solvent.[36] Second-row elements have always been considered to be more nucleophilic than those of the first row. Since much has been written about the relative nucleophilicity of phosphorus in solution, we include it here to complete the gas-phase trend. In the present study we do find that trimethylphosphine is far more reactive than Me_3N toward both *t*-BuOOH ($\Delta\Delta E^{\ddagger} = 15.0$ kcal/mol) and C4a-hydroperoxyflavin **3** ($\Delta\Delta E^{\ddagger} = 7.9$ kcal/mol). The oxygen atom transfer step for this highly exothermic reaction (−90.7 kcal/mol) comes much earlier along the reaction coordinate (TS-**6a**, Figure 7) with an O−P distance in the TS of 2.31 Å. In contrast, the overall reaction energy for the oxidation of Me_3N is only −5.3 kcal/mol. When the −OOH was afforded the opportunity for intramolecular H-bonding to O4 (TS-**6b**), we observed a slight increase in barrier as noted with the oxidation of DMS. The relative reactivity of the N and P nucleophiles toward FlHOOH **3** stands in marked contrast to the relative reactivities of these two nucleophiles toward the more reactive oxygen atom donor peroxyformic acid. The rate ratios for oxidation with **3** relative to *t*-BuOOH for N, S, Se, and P nucleophiles can be estimated from the calculated activation barriers to be 2×10^{12}, 4×10^{11}, 2×10^{11}, and 10^7.

We reported earlier[20] that Me_3N and Me_3P had nearly the same gas-phase barriers with peroxyformic acid ($\Delta\Delta E^{\ddagger} = 0.5$ kcal/mol, MP4//MP2/6-31G*) and that their relative reactivity in protic solvent is better attributed to a much greater ground-state solvation of the more basic tertiary amine than the polarizability of the phosphorus. In the present study we observed a 3.3 kcal/mol barrier difference with HCO_3H in favor of the P nucleophile at B3LYP/6-31+G(d,p) (3.0 and −0.3 kcal/mol, Table 2). Thus, the less reactive *t*-BuOOH is a more discriminating oxidant with a later TS and the difference in barrier heights for N versus P oxidation widens. These data also point out that rate differences should be compared for a common set of nucleophiles and that when you use oxidants of different reactivity you should anticipate different rate ratios. The differences in activation barriers for N versus P as well as S versus Se oxidation decrease markedly as the oxygen donor propensity of the oxidizing agent increases (*t*-BuOOH < flavinhydroperoxide < peracid).

Our theoretical data are quite consistent with the experimental[28] rate ratios for oxygen atom transfer from FlEtOOH. Native FADHOOH as modeled in this work by **3**, while intermediate in reactivity between a peracid and ROOH, is still capable of achieving the very difficult enzymatic oxidation of the benzene ring in *p*-hydroxybenzoic acid.[1] Since these data clearly demonstrate that native FlHOOH has only moderate reactivity as an oxygen atom donor, it would appear that some additional type of enzymatic catalysis might be required in order to effectively oxidize an aromatic ring. We are now looking at the possible catalytic role of other active-site residues in PHBH aromatic oxidation.

Conclusions

Comparative studies on relatively small peroxides support the treatment of more complex reaction systems involving O−O bond cleavage by the B3LYP/6-31+G(d,p) method. B3LYP is currently the most widely used, relatively fast computational method and these DFT data reproduce experimental values and the results of higher-level calculations [QCISD(T) and CASSCF] reasonably well, whereas HF and semiempirical AM1 methods, in the absence of electron correlation corrections, lead to unacceptable results. For example, model FlHOOH **3** shows an energy increase of 72.5 kcal/mol upon O−O bond elongation from 1.3 to 2.1 Å at the RAM1 level, yet its estimated O−O BDE is only ≈40 kcal/mol. We do emphasize that for late transition structures with O−O distances approaching 2 Å, the unrestricted (UB3LYP) protocol is recommended.

Oxidation reactions with heteroatom xenobiotics suggest that 4a-flavinhydroperoxide has a reactivity intermediate between that of *t*-BuOOH and a peracid. The intrinsic gas-phase reactivity of FlHOOH toward Me_3N and Me_2S is quite close ($\Delta\Delta E = 0.9$ kcal/mol), negating the suggestion that natural FMOs must increase the nucleophilicity of amines in some way in order to effect N-oxidation. Highly reactive oxygen atom donors such as peracids exhibit relatively small calculated differences in activation barriers for nucleophiles of different polarizability (e.g., Me_3N and Me_3P), while the less reactive more discriminating hydroperoxides (e.g., *t*-BuOOH) show much larger rate differences. Thus, this tendency has to be taken into account when simplified model systems are used in order to simulate the oxidation processes in flavoenzymes.

The computations on oxygen transfer from flavinhydroperoxide to Me_3N, Me_2S, Me_3P, and Me_2Se exhibit transition structures with $C_{4a}OOH\cdots O{=}C_4$ intramolecular hydrogen bonding in the flavinhydroperoxide. This reduces the absolute value of the imaginary frequency of the TS and in some cases the activation barrier. The magnitude of the imaginary frequency calculated at the same level of theory can serve as a convenient tool to estimate the extent of hydrogen atom displacement in the TS. For instance, it helps to distinguish between hydroxylation and oxygen transfer reactions. Oxygen atom transfer from FlHOOH produces a relatively stable alkoxide leaving group $FlHO^-$ ($pK_a \approx 9$) that reduces to some extent the necessity for stabilization by the 1,2-hydrogen shift and is therefore accompanied by a lowing of the imaginary frequency.

Acknowledgment. This work was supported by the National Science Foundation (CHE-0138632) and by National Computational Science Alliance under CHE990021N and utilized the NCSA SGI Origin2000 and University of Kentucky HP Superdome.

Supporting Information Available: Tables S1−S4, showing total energies of the isolated reactants and TSs; Cartesian coordinates of FlEtHOOH **1c** and FlHOOH **3** and TSs shown in Figures 4−10 [B3LYP/6-31+G(d,p)] and of the tBuOOH/Me_3P and tBuOOH/Me_3N prereaction complexes and corresponding TSs optimized at the B3LYP/6-31G(d) level; and Appendix (methodology of the KIE calculations). This material is available free of charge via the Internet at http://pubs.acs.org.

References and Notes

(1) (a) Walsh, C. In *Flavins and Flavoproteins*; Vincent, M., Williams, C. H., Eds.; Elsevier/North-Holland: Amsterdam, 1981; pp 121−132. (b)

Ballou, D. P. In *Flavins and Flavoproteins*; Vincent, M., Williams, C. H., Eds.; Elsevier/North-Holland: Amsterdam, 1982; p 301. (c) Bruice, T. C.In *Flavins and Flavoproteins*; Vincent, M., Williams, C. H., Eds.; Elsevier/North-Holland: Amsterdam, 1982; pp 265−277. (d) Wierenga, R. K.; Kalk, K. H.; van der Laan, J. M.; Drenth, J.; Hofsteenge J.; Weijer, W. J.; Jekel, P. A.; Beintema, J. J.; Muller, F.; van Berkel, W. J. In *Flavins and Flavoproteins*; Vincent, M., Williams, C. H., Eds.; Elsevier/North-Holland: Amsterdam, 1982; pp 11−18. (e) Bruice, T. C. In *Flavins and Flavoproteins*; Vincent, M., Williams, C. H., Eds.; Elsevier/North-Holland: Amsterdam, 1984; pp 57−60. (f) Walsh, C. In *Enzymatic Reaction Mechanisms*; W. H. Freeman and Co.: San Francisco, CA, 1979; pp 406−463.

(2) Ballou, D. P. In *Flavins and Flavoproteins*; Bray, R. C., Engel, P. C., Mayhew, S. G., Eds.; Walter de Gruyter: Berlin, 1984; pp 605−618.

(3) Müller, F. *Biochem. Soc. Trans.* **1985**, *13*, 443.

(4) (a) Entsch, B. *Methods Enzymol*. **1990**, *188*, 138. (b) Ortiz-Maldonado, M.; Aeschliman, S. M.; Ballou, D. P.; Massey, V. *Biochemistry* **2001**, *40* (30), 8705.

(5) Massey, V.; Schopfer, L. M.; Andreson, R. F. In *Oxidases and Related Systems*; King, T. E., Mason, H. S., Morrison, M., Eds.; Alan R. Liss: New York, 1988; pp 147−166.

(6) (a) Schreuder, H. A.; Van der Laan, J. M.; Hol, W. G. J.; Drenth, J. *J. Mol. Biol.* **1988**, *199* (4), 637. (b) Schreuder, H. A.; Prick, P. A. J.; Wierenga, R. K.; Vriend, G.; Wilson, K. S.; Hol, W. G. J.; Drenth, J. *J. Mol. Biol.* **1989**, *208* (4), 679.

(7) Schreuder, H. A.; Hol, W. G. J.; Drenth, J. *Biochemistry* **1990**, *29* (12), 3101.

(8) (a) Van der Laan, J. M.; Swarte, M. B. A.; Gronendijk, H.; Hol, W. G. J.; Drenth, J. *Eur. J. Biochem.* **1989**, *179* (3), 715. (b) van der Laan, J. M.; Schreuder, H. A.; Swarte, M. B. A.; Wierenga, R. K.; Kalk, K. H.; Hol, W. G. J.; Drenth, J. *Biochemistry* **1989**, *28* (18), 7199. (c) Schreuder, H. A.; van der Laan, J. M.; Swarte, M. B. A.; Kalk, K. H.; Hol, W. G. J.; Drenth, *Proteins: Struct., Funct., Genet.* **1992**, *14* (2), 178.

(9) (a) van Berkel, W. J. H.; Eppink, M. H. M.; Schreuder, H. A. *Protein Sci*. **1994**, *3* (12), 2245. (b) Schreuder, H. A.; Mattevi, A.; Obmolova, G.; Kalk, K. H.; Hol, W. G. J.; van der Bolt, F. J. T.; van Berkel, W. J. H. *Biochemistry* **1994**, *33* (33), 10161. (c) Lah, M. S.; Palfey, B. A.; Schreuder, H. A.; Ludwig, M. L. *Biochemistry* **1994**, *33* (6), 1555. (d) Jadan, A. P.; van Berkel, W. J. H.; Golovleva, L. A.; Golovlev, E. L. *Biochemistry (Moscow)* **2001**, *66* (8), 898.

(10) (a) Entsch, B.; Palfey, B. A.; Ballou, D. P.; Massey, V. *J. Biol. Chem*. **1991**, *266* (26), 17341. (b) Gatti, D. L., Entsch, B.; Ballou, D. P.; Ludwig, M. L. *Biochemistry* **1996**, *35* (2), 567.

(11) Anderson, R. F. In *Flavins and Flavoproteins*; Bray, R. C., Engel, P. C., Mayhew, S. G., Eds.; Walter de Gruyter: Berlin, 1984; pp 57−60.

(12) van Berkel, W. J.; Muller, F.; Jekel, P. A.; Weijer, W. J.; Schreuder, H. A.; Wierenga, R. K. *Eur. J. Biochem.* **1988**, *176* (2), 449.

(13) Vervoort, J.; Rietjens, I. M. C. M.; Vanberkel, W. J. H.; Veeger, C. *Eur. J. Biochem*. **1992**, *206* (2), 479.

(14) Perakyla, M.; Pakkanen, T. A. *J. Am. Chem. Soc*. **1993**, *115* (23), 10958.

(15) Canepa, C.; Bach, R. D.; Dmitrenko, O. *J. Org. Chem.* **2002**, *67*, 8653.

(16) (a) Ridder, L.; Mulholland, A. J.; Rietjens, I. M. C. M.; Vervoort, J. *J. Am. Chem. Soc*. **2000**, *122* (36), 8728. (b) Ridder, L.; Mulholland, A. J.; Vervoort, J.; Rietjens, I. M. C. M. *J. Am. Chem. Soc*. **1998**, *120* (30), 7641. (c) Ridder, L.; Palfey, B. A.; Vervoort, J.; Rietjens I. M. C. M. *FEBS Lett*. **2000**, *478* (1−2), 197.

(17) Billeter, S. R.; Hanser, C. F. W.; Mordasini, T. Z.; Scholten, M.; Thiel, W.; van Gunsteren, W. F. *Phys. Chem. Chem. Phys*. **2001**, *3* (5), 688.

(18) (a) Ziegler, D. M. *Annu. Rev. Pharmacol. Toxicol*. **1993**, *33*, 179. (b) Poulsen, L. L.; Ziegler, D. M. *Chem.-Biol. Interact.* **1995**, *96*, 57. (c) Ziegler, D. M. *Drug Metab. Rev.* **2002**, *34*, 503.

(19) Jones, K. C. Nature of the 4a-flavin hydroperoxide of microsomal flavin-containing monooxygenases; Doctoral Dissertation in Biological Chemistry, University Microfilms Int. No. DA8520922, University of Michigan, 1985.

(20) Bach, R. D.; Winter, J. E.; Mcdouall, J. J. W. *J. Am. Chem. Soc*. **1995**, *117* (*33*), 8586.

(21) (a) Frisch, M. J.; Trucks, G. W.; Schlegel, H. B.; Scuseria, G. E.; Robb, M. A.; Cheeseman, J. R.; Zakrzewski, V. G.; Montgomery, J. A.; Stratmann, R. E.; Burant, J. C.; Dapprich, S.; Millam, J. M.; Daniels, A. D.; Kudin, K. N.; Strain, M. C.; Farkas, O.; Tomasi, J.; Barone, V.; Cossi, M.; Cammi, R.; Mennucci, B.; Pomelli, C.; Adamo, C.; Clifford, S.; Ochterski, J.; Petersson, G. A.; Ayala, P. Y.; Cui, Q.; Morokuma, K.; Malick, D. K.; Rabuck, A. D.; Raghavachari, K.; Foresman, J. B.; Cioslowski, J.; Ortiz, J. V.; Baboul, A. G.; Stefanov, B. B.; Liu, G.; Liashenko, A.; Piskorz, P.; Komaromi, I.; Gomperts, R.; Martin, R. L.; Fox, D. J.; Keith, T.; Al-Laham, M. A.; Peng, C. Y.; Nanayakkara, A.; Gonzalez, C.; Challacombe, M.; Gill, P. M. W.; Johnson, B.; Chen, W.; Wong, M. W.; Andres, J. L.; Gonzalez, C.; Head-Gordon, M.; Replogle, E. S.; Pople, J. A. Gaussian 98, Revision A.7; Gaussian, Inc.: Pittsburgh, PA, 1998. (b) Curtiss, L. A.; Raghavachari, K.; Trucks, G. W.; Pople, J. A. *J. Chem. Phys.* **1991**, *94*, 7221. (c) Ochterski, J. W.; Petersson, G. A.; Montgomery, J. A. *J. Chem. Phys.* **1996**, *104*, 2598. (d) Barone, V.; Cossi, M.; Tomasi, J. *J. Comput. Chem.* **1998**, *19*, 404.

(22) (a) Schlegel, H. B. *J. Comput. Chem.* **1982**, *3*, 214. (b) Schlegel, H. B. *Adv. Chem. Phys.* **1987**, *67* (Pt. 1), 249. (c) Schlegel, H. B. In *Modern Electronic Structure Theory*; Yarkony, D. R., Ed.; World Scientific: Singapore, 1995; p 459.

(23) (a) Becke, A. D. *Phys. Rev. A* **1988**, *38*, 3098. (b) Lee, C.; Yang, W.; Parr, R. G. *Phys. Rev. B* **1988**, *37*, 785.

(24) (a) Becke, A. D. *J. Chem. Phys.* **1993**, *98*, 5648. (b) Stevens, P. J.; Devlin, F. J.; Chabalowski, C. F.; Frisch, M. J. *J. Phys. Chem.* **1994**, *98*, 11623.

(25) (a) CHARMM, version 24bl, 1995; Professor M. Karplus, Department of Chemistry, Harvard University, 12 Oxford St., Cambridge, MA 02138. (b) Gunsteren, W. F. van; Billeter, S. R.; Eising, A. A.; Hunenberger, P. H.; Kruger, P.; Mark, A. E.; Scott, W. R. P.; Tironi, I. G. *Biomolecular Simulation: The GROMOS96 Manual and User Guide*; Biomos b.v.: Zurich and Groningen, 1996.

(26) (a) Bach, R. D.; Owensby, A. L.; Gonzalez, C.; Schlegel, H. B. *J. Am. Chem. Soc*. **1991**, *113* (6), 2338. (b) Bach, R. D.; Su, M.-D. *J. Am. Chem. Soc.* **1994**, *116* (12), 5392. (c) Bach, R. D.; Glukhovtsev, M. N.; Gonzalez, C.; Marquez, M.; Estevez, C. M.; Baboul, A. G.; Schlegel, H. B. *J. Phys. Chem. A* **1997**, *101* (34), 6092. (d) Bach, R. D.; Glukhovtsev, M. N.; Gonzalez, C. *J. Am. Chem. Soc*. **1998**, *120*, 9902. (e) Bach, R. D.; Canepa, C.; Glukhovtsev, M. N. *J. Am. Chem. Soc*. **1999**, *121*, 6542. (f) Bach, R. D.; Dmitrenko, O.; Adam, W.; Schambony, S. *J. Am. Chem. Soc* **2003**, *125*, 924.

(27) (a) Estevez, C. M.; Dmitrenko, O.; Winter, J. E.; Bach, R. D. *J. Org. Chem*. **2000**, *65*, 8629. (b) Bach, R. D.; Ayala, P. Y.; Schlegel, H. B. *J. Am. Chem. Soc.* **1996**, *118*, 12758.

(28) (a) Kozlov, N. A.; Rabinovich, I. B. *Trudy Po Khim. I Khimicheeskoi Tekhnol*. **1964**, 189. (b) Reints, W.; Pratt, D. A.; Korth, H.-G.; Mulder, P. *J. Phys. Chem. A* **2000**, *104*, 10713.

(29) (a) Merenyi, G.; Lind, J.; Anderson, R. F. *J. Am. Chem. Soc*. **1991**, *113* (24), 9371. (b) Merenyi, G.; Lind, J. *J. Am. Chem. Soc.* **1991**, *113* (8), 3146.

(30) (a) Ball, S.; Bruice, T. C. *J. Am. Chem. Soc.* **1979**, *101*, 4017. (b) Ball, S.; Bruice, T. C. *J. Am. Chem. Soc.* **1980**, *102*, 6498. (c) Bruice, T. C.; Noar, J. B.; Ball, S.; Venkataram, U. V. *J. Am. Chem. Soc.* **1983**, *105*, 2452. (d) Bruice, T. C. *J. Chem. Soc., Chem. Commun.* **1983**, 14.

(31) van Berkel, W. J. H.; Muller, F. **1989**, *179*, 307.

(32) Bach, R. D. In Adam, W.; Degen, H.-G.; Pastor, A.; Saha-Möller, C. R.; Schambony, S. B.; Zhao, C.-G. Preparative Use of Peroxidic Oxidants for Oxygen-Transfer Reactions. In *DFG Research Report on Peroxide Chemistry: Mechanistic and Preparative Aspects of Oxygen Transfer*; Adam, W., Saha-Möller, C. R., Eds.; Wiley-VCH: Weinheim, Germany, 2000.

(33) For a discussion of solvent-assisted proton transfer in alkyl hydrogen peroxides, see Dankleff, M. A. P.; Ruggero, C.; Edwards, J. O.; Pyun, H. Y. *J. Am. Chem. Soc.* **1968**, *90*, 3209.

(34) Bach, R. D.; Dmitrenko, O. *J. Am. Chem. Soc*. **2003** (submitted for publication).

(35) Beaty, N.; Ballou, D. *J. Biol. Chem.* **1981**, *256*, 4611 and 4619.

(36) (a) Carey, F. A.; Sundberg, R. J. *Advanced Organic Chemistry*, 3rd ed.; Plenum Press: New York, 1990; Part A, p 284. (b) Lowry, T. H.; Richardson, K. S. *Mechanism and Theory in Organic Chemistry*, 3rd ed.; Harper & Row: New York, 1987; p 367.